Applied Surface Science 257 (2011) 6264–6269

Contents lists available at ScienceDirect

Applied Surface Science

journal homepage: www.elsevier.com/locate/apsusc

Anti-icing performance of superhydrophobic surfaces

S. Farhadi, M. Farzaneh[1], S.A. Kulinich*

CIGELE/INGIVRE, Department of Applied Sciences, Université du Québec à Chicoutimi, 555 University blvd., Saguenay, PQ, Canada G7H 2B1

ARTICLE INFO

Article history:
Received 14 December 2010
Received in revised form 12 February 2011
Accepted 13 February 2011
Available online 18 February 2011

PACS:
68.35.Md
68.08.Bc
82.45.Mp

Keywords:
Ice adhesion
Ice repellency
Superhydrophobicity
Ice adhesion strength
Roughness
Water condensation
Durability

ABSTRACT

This article studies the anti-ice performance of several micro/nano-rough hydrophobic coatings with different surface chemistry and topography. The coatings were prepared by spin-coating or dip coating and used organosilane, fluoropolymer or silicone rubber as a top layer. Artificially created glaze ice, similar to the naturally accreted one, was deposited on the nanostructured surfaces by spraying supercooled water microdroplets (average size ~80 μm) in a wind tunnel at subzero temperature (−10 °C). The ice adhesion strength was evaluated by spinning the samples in a centrifuge at constantly increasing speed until ice delamination occurred. The results show that the anti-icing properties of the tested materials deteriorate, as their surface asperities seem to be gradually broken during icing/de-icing cycles. Therefore, the durability of anti-icing properties appears to be an important point for further research. It is also shown that the anti-icing efficiency of the tested superhydrophobic surfaces is significantly lower in a humid atmosphere, as water condensation both on top and between surface asperities takes place, leading to high values of ice adhesion strength. This implies that superhydrophobic surfaces may not always be ice-phobic in the presence of humidity, which can limit their wide use as anti-icing materials.

1. Introduction

Ice and wet-snow adhesion and excessive accumulation on exposed structures and equipment is well known to cause serious problems in cold-climate regions [1–4]. Atmospheric icing occurs when super-cooled water droplets (or snow particles) come into contact with the surface of exposed structures, which may lead to material damage and socioeconomic costs in many sectors of the economy, including power transmission and distribution, telecommunication networks, aircraft, boats, etc. [2,3]. Each year, numerous failures due to ice accumulation are reported in Iceland, Norway, Canada, Finland, the US, Russia, and even in Japan and China [1–5]. To counter this problem, various de-icing and anti-icing techniques have been developed over the past few decades [2,3]. Among those, ice-repellent coatings have been recently proposed as a passive technique to reduce or prevent ice accumulation on the outdoor structures. Such coatings provide reduced adhesion or delay water freezing on their surface [5–14], which is expected to result in lower ice or wet-snow accumulation on such coated surfaces [7,15]. Therefore, the research on coatings capable of reducing wet-snow, frost, or ice accumulation has been going on for several decades [5–25].

Superhydrophobic surfaces, i.e. those characterized by water contact angle (CA) above 150° and low CA hysteresis (CAH), were first tested by Saito et al. [5] and showed promising anti-icing performance. More recently, other groups showed reduced ice adhesion [6,8,11–13] or delayed water freezing [7,24,26,27] on rough superhydrophobic surfaces. These two characteristics make superhydrophobic surfaces attractive candidates for anti-ice applications, i.e. where reduced ice/snow accumulation is needed. However, the ice-releasing performance of rough superhydrophobic surfaces has not been adequately studied yet in different conditions.

In this work, we prepared several nanostructured superhydrophobic coatings with different chemistry and topography and tested them as anti-ice candidate materials. The glaze ice accumulated on the samples was prepared by spraying supercooled water microdroplets in a wind tunnel at subzero temperatures. Such conditions thus simulated most severe natural atmospheric icing. The samples were tested over numerous icing/de-icing cycles in order to assess the durability of their ice-releasing performance. Also, ice adhesion was evaluated on the samples previously placed on a cold surface to condense water, i.e. on 'wet' surfaces.

* Corresponding author.
E-mail address: skulinic@uqac.ca (S.A. Kulinich).
[1] Tel.: +1 418 545 5044; fax: +1 418 545 5032.

0169-4332/$ – see front matter.
doi:10.1016/j.apsusc.2011.02.057

Table 1
Preparation and properties of the samples used in this work.

Sample	Description	Preparation	CA (°)	CAH (°)
A	CeO_2–Zonyl 8740	Spin-coating	152.4 ± 2.6	5.7 ± 2.0
B	FAS-13	Etching/dip-coating	153.2 ± 2.4	6.1 ± 1.7
C	Ag–Zonyl 8740	Spin-coating/anneal/dip-coating	155.1 ± 1.8	5.3 ± 1.9
D	TiO_2–RTV SR	Etching/spin-coating	154.8 ± 2.1	6.8 ± 1.5

2. Experimental

Table 1 gives a brief description of the samples prepared and tested in this study. Aluminium alloy (AA6061) plates, 3.2 cm × 5.0 cm in size, were used as substrates. Sample A was prepared by spin-coating a CeO_2 nanopowder suspension in Zonyl 8740 (perfluoroalkyl methacrylic copolymer soluble in water, DuPont). This process has been already described somewhere [6,8,28]. In brief, CeO_2 nanopowder, with particle size <50 nm from Aldrich (8.0 g), was mixed with 80 ml of deionized water. The suspension was sonicated for 30 min, after which 5.0 ml of Zonyl 8740 was added. The final suspension was stirred for 3 h before being coated on the substrate.

Sample B was a plate of etched aluminium coated with 1H,1H,2H,2H-perfluoro-octyltriethoxysilane (FAS-13, from Aldrich). The plate was first etched in 17% HCl for 5 min, after which it was sonicated in deionized water, rinsed and dried in air for 1 h. A methanol solution of FAS-13 was hydrolyzed by the addition of a 3-fold molar excess of water at room temperature. The etched metallic substrate was immersed in the hydrolyzed silane solution for 1 h at room temperature, then rinsed in methanol and heat treated at 80 °C for 2 h. The procedure has been described in greater detail elsewhere [29].

Sample C was spin-coated by using a methanol/ethyleneglycol (20:1, v/v) suspension of Ag nanoparticles (100–600 nm in size, prepared following the recipe in Ref. [30]), after which the coating was annealed (2 h at 200 °C in air), dip-coated in a water–Zonyl 8740 (10:1, v/v) solution for 1 h, and finally dried in air at 100 °C for 3 h to remove any volatile components. This sample was expected not to be mechanically strong as its rough structures (Fig. 1c) were based on relatively loose Ag nanoparticles sintered during annealing to better bond to each other followed by passivating the final rough coating with a thin fluoropolymer later.

Nanostructured superhydrophobic sample D was prepared by spin-coating a suspension of room-temperature-vulcanized silicone rubber (RTV SR, from Dow Corning) in hexane (1:3, v/v) doped with 3% of TiO_2 nanoparticles (smaller than 100 nm, from Aldrich) over the substrate surface uniformly and letting it dry at ~80 °C for 3 h. The procedure was also adopted from Refs. [6,8,28] and then slightly modified.

The wettability results reported in Table 1 were collected by using a DSA-100 contact angle goniometer from Krüss. Surface topographies were analyzed with a scanning electron microscopy (SEM, LEO Gemini instrument) and atomic force microscopy (AFM, Escope from Veeco). The ice adhesion evaluation tests were conducted on Al beams with 1-cm thick glaze ice samples spun in a home-made centrifuge apparatus placed in a cold room at −10 °C [6,8,11–13]. The samples attached to the beams were previously iced in a wind tunnel, then placed in the centrifuge and spun there with increasing rotational speed until ice detachment occurred [6,8,11–13]. It was verified that the iced sample type and geometry would not allow cohesion failure, and provided well reproducible results during de-icing. Ice mass and area were carefully evaluated both before and after de-icing. The procedure to evaluate the ice adhesion strength (as the shear stress of ice detachment) was previously reported in greater detail elsewhere [6,8,11–13]. Three duplicates were prepared for each sample in Table 1, and the results were calculated as the average of the three. Further details on this technique can be found in recent reports [6,8,11–13].

3. Results and discussion

Fig. 1 shows the surface images of samples A–D, and Table 1 exhibits both CA and CAH values of the samples. All the samples were found to be rough at micro/nano-scale. Thus, air was expected to entrap into such structures during wetting. As a result, the Cassie wetting mode was expected for these samples with high surface roughness and low-energy top layers [7,14,19,23,31–34]. The water–solid contact area on these samples was expected to be small, which is consistent with the small CAH values (~5–7°) and high CA values (above 150°) listed in Table 1. This is shown in Fig. 2, where the wetting of a rough hydrophobic surface in the Cassie wetting regime is schematically illustrated. Fig. 2 shows that in the Cassie regime, a large amount of air entrapment in the surface irregularities on a rough hydrophobic surface leads to a very small area of the surface which is in contact with the water drop. As a result, such surfaces are often referred as 'slippy', as water drops are very mobile on them.

Reports on how hydrophobic and superhydrophobic surfaces perform at temperatures ≤0 °C are relatively seldom in the literature [6–8,15]. Moreover, while numerous reports appear which discuss dynamic behaviour of water droplets in relation to surface topography (asperities height, shape, regularities and spacing) [31,35,36], the behaviour of rough hydrophobic surfaces during icing and de-icing (in particular, under different conditions) is largely unknown. Recently, several groups have reported the water repellency of superhydrophobic surfaces to be external-condition-dependent, as it deteriorates when water condenses in the rough structures around the freezing point [32,34,37–41]. This implies that extensive and systematical experimental investigations of such surfaces under different icing conditions (in particular at temperatures close to or below 0 °C) are needed in order to develop reliable and efficient anti-ice materials.

Therefore, we first put our samples on a Peltier cooling stage to condense atmospheric water and make them 'wet', after which their hydrophobic and ice-releasing properties were evaluated and compared with those of 'dry' (i.e. as-prepared) surfaces. Fig. 3 demonstrates how wetting behaviour of sample B changed after water was condensed on its surface at ~0 °C. It is clearly seen in Fig. 3b and d that, compared to the 'dry' surface in Fig. 3a and c, the CA decreased and CAH increased on the 'wet' surface, making it still hydrophobic but 'sticky' for water. This finding is well consistent with the previous reports by others who also observed significant deterioration in the hydrophobicity of 'wet' superhydrophobic surfaces (increased CAH and decreased CA values) caused by water condensation from air [32,34,37–41]. When 'wet' sample B was iced (after 2 h of water condensation), the measured value of shear stress of ice detachment on its surface was measured to be ~150 kPa. This is about three times larger than a similar value obtained on the 'dry' (i.e. as-prepared) sample B, which was ~55 kPa (see Fig. 4b). Similar results were obtained for the other samples. The extent to which ice adhesion strength increased on the surface of samples depended on several parameters, including the duration of water condensation and surface temperature. In all cases, however, an increase in ice adhesion strength was observed after the samples were kept in air for a certain period of time at temperatures close or below zero. This implies that the use of superhydrophobic surfaces may be limited

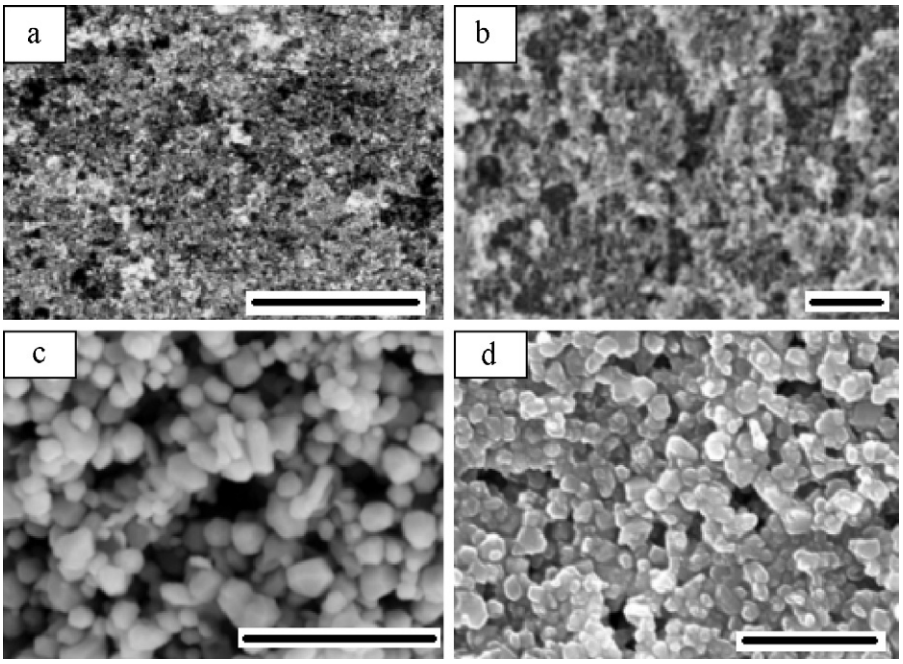

Fig. 1. SEM images of super-hydrophobic samples used in this study. (a) Spin-coated CeO_2–Zonyl 8740 based sample. (b) Etched Al sample passivated with FAS-13. (c) Spin-coated Ag nano-particles, followed by annealing and subsequent dip-coating with a thin film of Zonyl 8740. (d) Etched Al spin-coated with TiO_2–silicone rubber suspension in n-hexane. The scale bars indicate 5 μm (b and d) and 2 μm (a and c).

in a humid atmosphere since they lose their anti-ice efficiency and become, partially, ice-philic.

The most recent reports by others [16,17] are in good agreement with the above finding. Varanasi et al. [16] studied frost formation on superhydrophobic surfaces and how it impacts their anti-ice properties. As frost was shown to form indiscriminately on the material rough structures, this led to significantly increased ice adhesion [16]. Yang et al. [17] also reported that water condensation (from atmospheric humidity) led to increased ice adhesion on fluoropolymer surfaces with submicron roughness. The authors also attributed this to water condensed in the rough structures [17]. These two recent reports thus give support to our conclusion on the limited use of superhydrophobic coatings as anti-ice materials in a humid atmosphere. Depending on ambient conditions, water condensation or frost formation may occur on their rough structures, but in both cases this will lead to a significant deterioration of anti-ice performance of the surfaces.

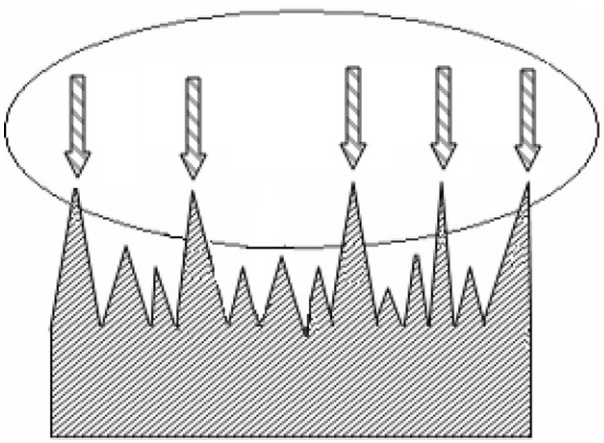

Fig. 2. Schematic presentation of a water droplet sitting atop a superhydrophobic surface (Cassie wetting mode). Arrows indicate surface asperities which are likely to be indented into ice when the droplet solidifies.

Figs. 4 and 5 present the shear stresses of ice detachment values of the 'dry' samples as a function of the number of icing/de-icing cycles. The average value of shear stresses of ice detachment obtained on uncoated mirror-polished aluminium (not shown) was $\sim 362 \pm 26$ kPa. In agreement with the previous studies on low-CAH superhydrophobic surfaces [6,8], the initial values of shear stress of ice detachment on the as-prepared samples were ~3.3–6.6 times lower than those on the polished aluminium standard (being ~55–110 kPa, Figs. 4 and 5), which is consistent with the above mentioned Cassie wetting regime on their surfaces (see Fig. 2) that eventually led to small ice-solid contact areas [6,8].

However, having being iced/de-iced repetitively, the samples showed gradually increased ice adherence (see Figs. 4 and 5). For instance, after eleven icing/de-icing experiments, samples A, B, and D demonstrated ice adhesion strengths increased by a factor of about 1.8–2.4 if compared with the as-prepared surfaces (Figs. 4 and 5b). Meanwhile, sample C demonstrated an approximately three-fold increase in ice adhesion strength on its surface already after only as many as five icing/shedding events (Fig. 5a). Based on the previous reports on various superhydrophobic surfaces [6,8], this increase in ice adhesion strength values is believed to be associated with a larger ice-solid contact area on these nanostructured surfaces after several icing/de-icing events.

To better understand these observations, we performed AFM surface analyses of samples A and B after the de-icing experiments in order to examine the changes (if any) in sample topographies. Root-mean-square roughness (R_{rms}) was evaluated over several different locations on both samples, and the results are presented in Fig. 6 as a function of the number of icing/de-icing events. A small decrease in surface roughness appears to be seen for sample B, which corresponds well to the slightly changed ice adhesion strength on this sample over eleven icing/de-icing cycles (Fig. 4b). At the same time, a somewhat larger decrease in surface roughness was observed for sample A, which can be associated with a more remarkable increase in ice adhesion strength on this nanostructured surface during the subsequent icing/de-icing cycles (Fig. 4a).

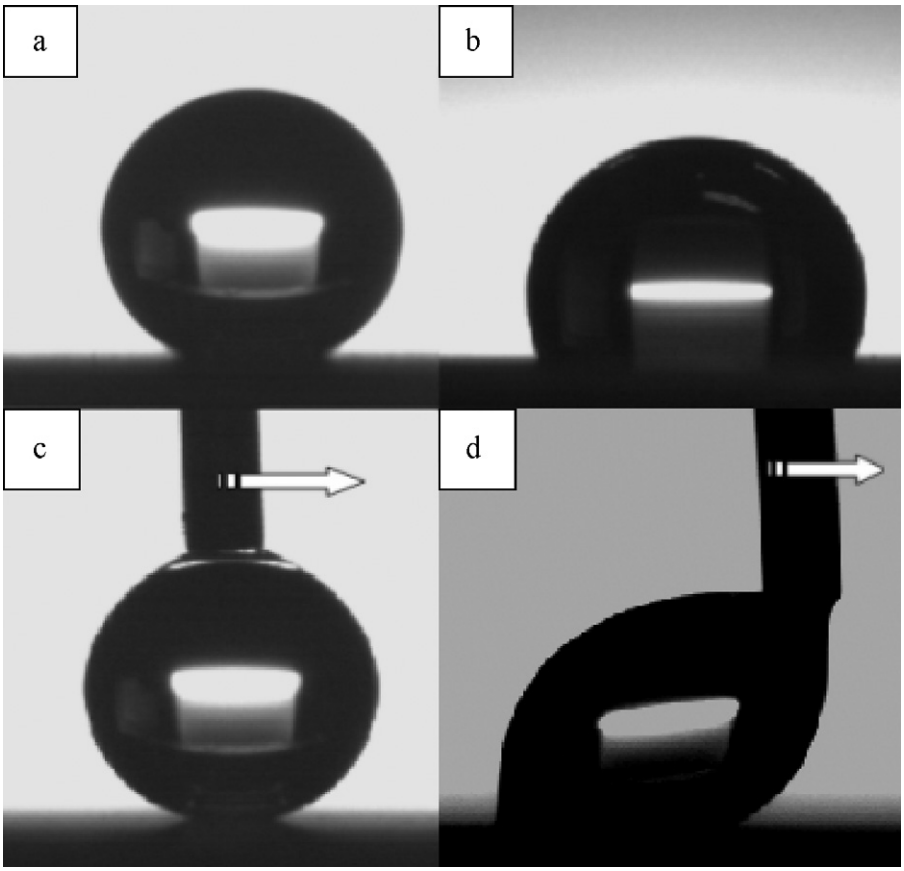

Fig. 3. Images of water droplets on FAS-coated sample (sample B). (a) and (c) As-prepared ('dry') sample; (b) and (d) after water condensation ('wet' surface) for 3 h at ~0 °C. Static (a),(b) and moving (c),(d) droplets are shown.

These decreases in surface roughness (Fig. 6) correlate well with the increase in ice adhesion strength on these samples, as observed in Fig. 4.

In parallel, CA values were also measured on the samples between icing/de-icing experiments, and the results are presented in Figs. 4 and 5. It is well seen that water repellency of all the samples increasingly deteriorated as the samples were repeatedly iced/shed. The results presented in Figs. 4–6 permit to assume that the increased ice adhesion strength, somewhat deteriorated water repellency and somewhat decreased surface roughness of the repeatedly iced/de-iced samples can be related to a gradual damage of the rough structures of the sample surfaces. As the surface roughness of the samples decreased, consequently, partial switch of the wetting regime from a pure Cassie (with low CAH and high CA values) to a mixed Wenzel–Cassie regime was expected on such surfaces, which had to cause the observed gradual increase in ice adhesion strength [6,8,28].

The rough nanostructured superhydrophobic surfaces in this study are therefore shown to demonstrate time-dependent ice-releasing performances. Their sharp tips schematically shown in Fig. 2 could be (partially) broken and removed by ice during de-icing as they were believed to be indented into ice to some degree. Moreover, some damage could also be caused by icing, because the water expansion on the solid surface caused by freezing can induce a very significant interfacial stress. This assumption is in good agreement with the gradual decrease in surface roughness observed for the samples over icing/shedding tests (Fig. 6). The fact that rough surface asperities get indented into liquid (including frozen liquid) and their tips can be damaged during the solidification of the liquid has been recently confirmed by Ensikat and coworkers [33]. The cryo-SEM observations of frozen droplets on both micro- and nano-structured surfaces demonstrated that asperities of both natural and artificial surfaces were indented into frozen liquids and, as a result, their tips remained partially embedded into the liquids on the droplet removal, thus damaging the asperities [33].

Because the samples used in this work had different mechanical properties, their resistance to damage during icing/de-icing (abrasive resistance) was expected to be different. And indeed, Fig. 5a shows that sample C, whose rough structures were based on practically loose Ag nanoparticles (bound to each other via annealing and, to some degree, by a fluoropolymer layer), deteriorated very quickly. After only five icing/shedding experiments, its water repellency was significantly lower, while ice adhesion strength on its surface was roughly close to that on mirror-polished aluminium. Samples A, B and D showed remarkably lower deterioration rates (and consequently – higher abrasive resistance) during icing/de-icing cycles, which could be expected since these samples had much firmer and stronger surface asperities. However, all the samples were gradually affected by repetitive icing/de-icing tests, demonstrating a relatively poor abrasive resistance and, as a result, increasingly deteriorating ice-repellent performance.

Therefore, abrasive resistance over icing/de-icing cycles should be thoroughly tested, while developing superhydrophobic materials for anti-icing applications outdoors. This implies that the mechanical properties of the candidate coatings must be taken into account and their performance over repeated icing/de-icing cycles systematically studied. Based on the findings of the present study, it can be anticipated that superhydrophobic surfaces made of very rigid or very elastic materials can demonstrate improved abrasive resistance against icing/de-icing, which is still to be experimentally proven.

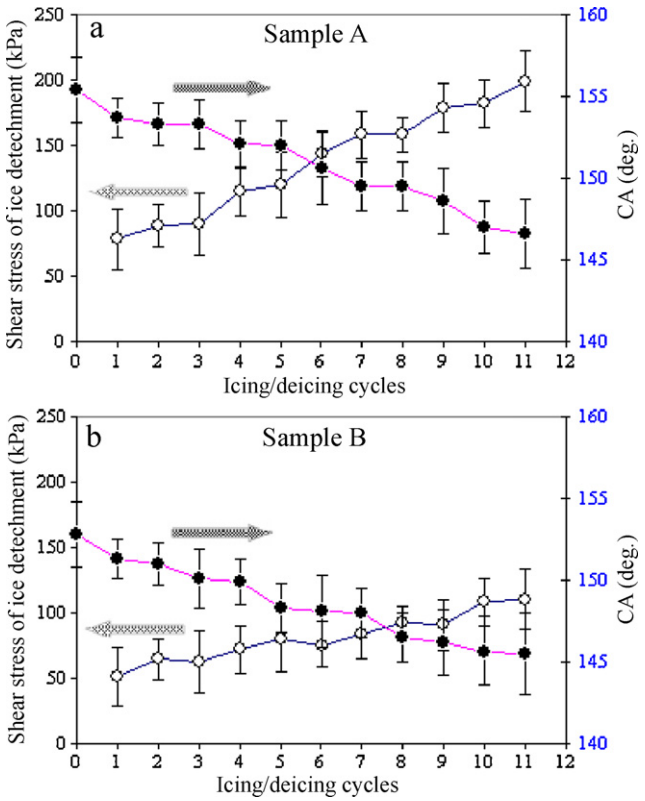

Fig. 4. Shear stress of ice detachment (open symbols) and contact angle (filled symbols) versus icing/de-icing cycles. (a) CeO_2–Zonyl 8740 sample, (b) FAS-13 passivated sample. Lines are only given as guides to the eye.

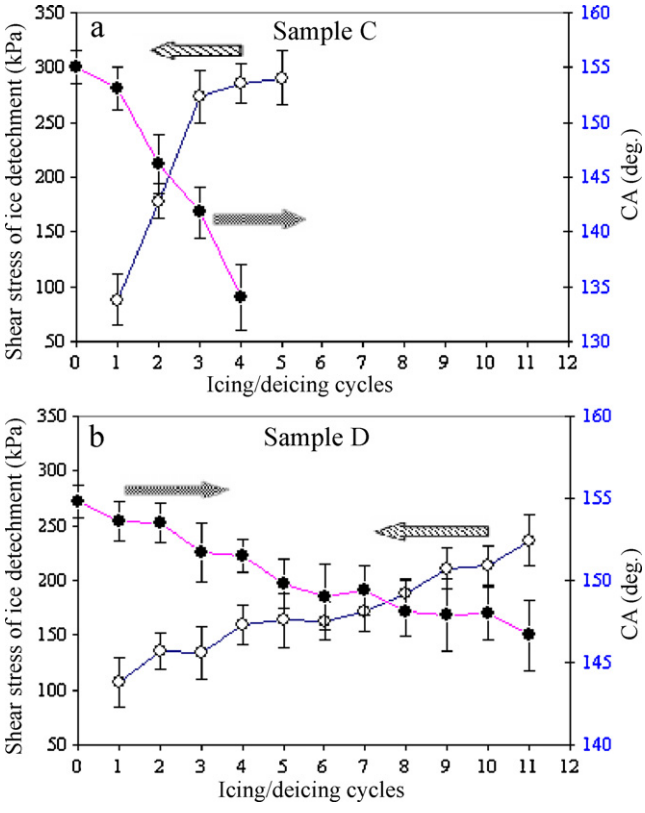

Fig. 5. Shear stress of ice detachment (open symbols) and contact angle (filled symbols) versus icing/de-icing cycles. (a) Ag–Zonyl 8740 sample, (b) TiO_2–silicone rubber coated sample. Lines are only given as guides to the eye.

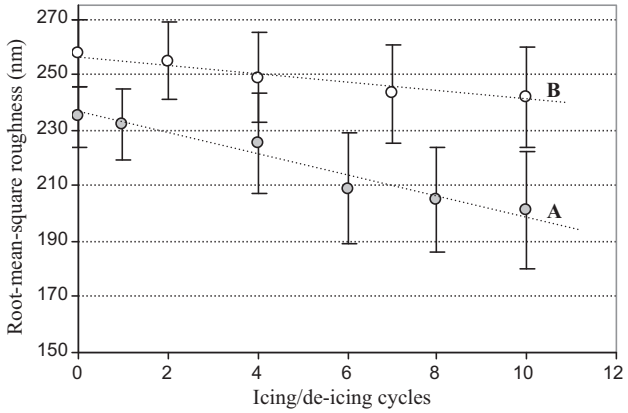

Fig. 6. Root-mean-square (R_{rms}) surface roughness of samples A and B as a function of icing/de-icing cycles. Lines are only given as guides to the eye.

4. Concluding remarks

This paper raises doubts about the wide use of nano-structured superhydrophobic coatings as universal anti-icing materials. We studied ice-repellent performance of several superhydrophobic coatings based on different materials, while the glaze ice used in tests was prepared under conditions similar to those in nature. The results of ice adhesion strength evaluation, after as many as eleven icing/de-icing cycles, showed that the anti-ice performance of the samples significantly deteriorated. Even though superhydrophobic surfaces tested in this study did exhibit significantly lower ice adhesion strengths than that on polish aluminium, their ice-releasing performance degraded gradually during icing and de-icing. Superhydrophobic materials with very hard or elastic rough structures are postulated to demonstrate a better durability under similar conditions. Moreover, when 'wet' (as a result of water condensation in the rough structures), the tested surfaces lost their ice repellency. This implies that the use of such coatings in humid environments may be limited.

Acknowledgments

The authors thank F. Arianpour (Univ. of Quebec) and Dr. A. Safaee (Queen's Univ.) for their help with some experiments.

References

[1] L.O. Andersson, C.G. Golander, S. Persson, J. Adhes. Sci. Technol. 8 (1994) 117–132.
[2] S. Frankenstein, A.M. Tuthill, J. Cold Reg. Eng. 16 (2002) 83–96.
[3] J.L. Laforte, M.A. Allaire, J. Laflamme, Atmos. Res. 46 (1998) 143–158.
[4] V.K. Croutch, R.A. Hartley, J. Coat. Technol. 64 (1992) 41–52.
[5] H. Saito, K. Takai, G. Yamauchi, Surf. Coat. Int. 80 (1997) 168–171.
[6] S.A. Kulinich, M. Farzaneh, Langmuir 25 (2009) 8854–8856.
[7] L.L. Cao, A.K. Jones, V.K. Sikka, J.Z. Wu, D. Gao, Langmuir 25 (2009) 12444–12448.
[8] S.A. Kulinich, M. Farzaneh, Appl. Surf. Sci. 255 (2009) 8153–8157.
[9] A.J. Meuler, J.D. Smith, K.K. Varanasi, J.M. Mabry, G.H. McKinley, R.E. Cohen, ACS Appl. Mater. Interfaces 2 (2010) 3100–3110.
[10] S.A. Kulinich, S. Farhadi, K. Nose, X.W. Du, Langmuir 27 (2011) 25–29.
[11] R. Menini, Z. Ghalmi, M. Farzaneh, Cold Reg. Sci. Technol. 65 (2011) 65–69.
[12] S.A. Kulinich, M. Farzaneh, Cold Reg. Sci. Technol. 65 (2011) 60–64.
[13] R. Menini, M. Farzaneh, Met. Finish. 107 (2009) 40–46.
[14] S.A. Kulinich, M. Farzaneh, Vacuum 79 (2005) 255–264.
[15] F.C. Wang, C.R. Li, Y.Z. Lv, F.C. Lv, Y.F. Du, Cold Reg. Sci. Technol. 62 (2010) 29–33.
[16] K.K. Varanasi, T. Deng, J.D. Smith, M. Hsu, N. Bhate, Appl. Phys. Lett. 97 (2010) 234102.
[17] S.Q. Yang, Q. Xia, L. Zhu, J. Xue, Q.J. Wang, Q.M. Chen, Appl. Surf. Sci. 257 (2011) 4956–4962.
[18] T. Kako, A. Nakajima, Z. Kato, K. Uematsu, T. Watanabe, K. Hashimoto, J. Ceram. Soc. Jpn. 110 (2002) 186–192 (in Japanese).
[19] S.A. Kulinich, M. Farzaneh, Appl. Surf. Sci. 230 (2004) 232–240.
[20] R. Karmouch, G.G. Ross, Appl. Surf. Sci. 257 (2010) 665–669.

[21] L. Yin, Q. Xia, J. Xue, S.Q. Yang, Q.J. Wang, Q.M. Chen, Appl. Surf. Sci. 256 (2010) 6764–6769.
[22] H. Murase, K. Nanishi, H. Kogure, T. Fujibayashi, K. Tamura, N. Haruta, J. Appl. Polym. Sci. 54 (1994) 2051–2062.
[23] S.A. Kulinich, M. Farzaneh, Surf. Sci. 573 (2004) 379–390.
[24] L. Mishchenko, B. Hatton, V. Bahadur, J.A. Taylor, T. Krupenkin, J. Aizenberg, ACS Nano 4 (2010) 7699–7707.
[25] H. Wang, L.M. Tang, X.M. Wu, W.T. Dai, Y.P. Qiu, Appl. Surf. Sci. 253 (2007) 8818–8824.
[26] M. He, J.X. Wang, H.L. Li, X.L. Jin, J.J. Wang, B.Q. Liu, Y.L. Song, Soft Matter 6 (2010) 2396–2399.
[27] P. Tourkine, M. Le Merrer, D. Quéré, Langmuir 25 (2009) 7214–7216.
[28] S.A. Kulinich, M. Farzaneh, Appl. Surf. Sci. 255 (2009) 4056–4060.
[29] B.T. Qian, Z.Q. Shen, Langmuir 21 (2005) 9007–9009.
[30] D. Kim, S. Jeong, J. Moon, Nanotechnology 17 (2006) 4019–4024.
[31] M. Miwa, A. Nakajima, A. Fujishima, K. Hashimoto, T. Watanabe, Langmuir 16 (2000) 5754–5760.
[32] K.A. Wier, T.J. McCarthy, Langmuir 22 (2006) 2433–2436.
[33] H.J. Ensikat, A.J. Schulte, K. Koch, W. Brthlott, Langmuir 25 (2009) 13077–13083.
[34] B. Mockenhaupt, H.-J. Ensikat, M. Spaeth, W. Barthlott, Langmuir 24 (2008) 13591–13597.
[35] D. Öner, T.J. McCarthy, Langmuir 16 (2000) 7777–7782.
[36] C.W. Extrand, Langmuir 22 (2006) 1711–1714.
[37] X.C. Xiao, Y.T. Cheng, B.W. Sheldon, J. Rankin, J. Mater. Res. 23 (2008) 2174–2178.
[38] R. Karmouch, G.G. Ross, J. Phys. Chem. C 114 (2010) 4063–4066.
[39] Y.T. Cheng, D.E. Rodak, A. Angelopoulos, T. Gacek, Appl. Phys. Lett. 87 (2005) 194112.
[40] R.D. Narhe, D.A. Beysens, Langmuir 23 (2007) 6486–6489.
[41] X.L. Tang, J.F. Dong, X.F. Li, J. Colloid Interface Sci. 325 (2008) 223–227.